Title
EXPERIMENTAL STUDY OF GAS-COOLED CURRENT LEADS FOR SUPERCONDUCTING MAGNETS

Author
Warren, Richard P.

Publication Date
1978-04-01

Experimental Study of Gas-Cooled Current Leads for Superconducting Magnets

Richard P. Warren

Lawrence Berkeley Laboratory
University of California
Berkeley, California 94720

ABSTRACT

Design details and experimental test results from several design variations of the gas-cooled, copper current leads used in conjunction with the superconducting dipole magnets for ESCAR (Experimental Superconducting Accelerator Ring) are reported. Thermal acoustic oscillations, which were experienced with an initial design, were eliminated in subsequent designs by a reduction of the hydraulic diameter. The occurrence of these oscillations is in general agreement with the stability analysis of Rott[1] but the observed gas flow dependence is not in agreement with some other recently reported results for leads operated with supercritical phase coolant.[2] An empirically determined correlation was obtained by plotting lead resistance vs. enthalpy gain of the coolant gas. The resulting family of curves can be reduced to a single line on a plot of effective resistivity vs. the product of current and cross-sectional area divided by the product of the square of the mass flow of the coolant and the lead length. This correlation, which should be applicable to other designs of copper current leads in which ideal heat transfer to the coolant gas is ap-

proached, predicts that the enthalpy gain of the coolant, and therefore the peak lead temperature, is proportional to the cube of the ratio of current to coolant mass flow. The effective value of the strongly temperature-dependent kinematic viscosity of the coolant gas was found to vary linearly with the effective resistivity of the lead.

INTRODUCTION

The ESCAR (Experimental Superconducting Accelerator Ring) is cooled with liquid helium supplied by a 1500-W refrigerator. The current lead coolant gas, which is returned to the refrigerator at ambient temperature, is budgeted at 3 g/s. The gas-cooled current lead set includes 12 (2000-A) dipole leads, 64 (500-A) quadrupole leads, and 200 (50-A) trim coil leads. With this large number of leads and limited coolant flow available, the primary design considerations are related to reliability and minimization of the required coolant mass flow. Cold-end heat conduction, while important, is relegated to a secondary consideration since it is not a large fraction of the available refrigeration.

LEAD DESIGN

The current is carried in thin plates of ETP copper which are closely spaced to form narrow rectangular flow passages for the coolant gas. The first design tried was made by folding an 0.0127-cm (0.005-in.) sheet accordion style to form narrow rectangular flow channels. The small dimension of the flow channels was 0.056 cm (0.022 in.). This lead worked quite well as long as the coolant gas flow was greater than about 0.1 g/s. At lower flows, thermal acoustic oscillations, which are predicted by the stability analysis of Reference 1, occurred with an attendant increase in the cold-end heat transfer by about one order of magnitude and very strong mechanical vibrations. The severity of oscillations seemed to increase with decreasing coolant flow. This flow dependence is contrary to that reported in Reference 2 where the oscillations in a supercritical system were found to cease at low or no flow. The stability analysis of Reference 1 is reproduced here on Figure 1 on the dimensionless coordinates suggested by Reference 3. The stability boundary for $\xi = 0.2$ is taken from Reference 2. The model assumes a long gas-filled tube, the temperature of which is assumed to be piece-wise constant with a step change between the two levels. The length of the cold end is ℓ_c and of the warm end ℓ_h. Their ratio, $\xi = \ell_h/\ell_c$, is a parameter of the stability curves. For the folded plate design the abscissa is about 35 so that for ξ in the range of 0.5 to 1 oscillations are predicted for temperature ratios greater than about 10, which is always the case.

In order to avoid the thermal acoustics and simplify the construction, a second design was built. A cross section is shown in Figure 2. Copper strips are hemmed along the edge, embossed periodically at the center, and stacked to form flow passages. Seven 0.0254-cm (0.010-in.) thick ETP copper strips are sandwiched between two 0.0127-cm (0.005-in.) strips. The thinner boundary conductors insure symmetrical heating of the 0.0254-cm-thick flow channels. This assembly is enclosed within a welded stainless steel jacket which is milled away along one edge over the lower 6 cm to allow direct attachment of the superconductor to the edges of the copper sheets. Referring to Figure 1, the dimensionless abscissa is about 16 for these leads. The design point thus falls very close to the predicted stability boundary. No thermal acoustic oscillations could be detected with these leads. The pressure drop, however, was excessive. In order to reduce the pressure drop, the tapered design shown in Figures 2 and 3 was built. The copper area on this design tapers from 0.70 cm^2 at the top to 0.37 cm^2 at the bottom. The flow passage width tapers from 1.92 cm at the top to 0.56 cm at the bottom. The small dimension of the flow passage was opened up to 0.032 cm (0.0125 in.), resulting in the design point number 3 shown on Figure 2 ($\Delta = 20$), which is within the unstable region. No thermal acoustic oscillations have been encountered, however.

EXPERIMENTAL METHODS

The leads are suspended vertically from the lid of an open mouth 25-cm (10-in.) diameter, 114-cm (45-in.) deep liquid nitrogen jacketed Dewar flask. The leads are connected at the cold end by a NbTi superconductor. Current is supplied at the warm end via water-cooled cables. Liquid level in the Dewar flask is monitored with a continuous-reading superconducting level gauge. The Dewar flask vent flow can be circuited either through the current leads or can bypass the leads or any combination of the two. Vent rate is read on a buoyant ball flow meter.

EXPERIMENTAL RESULTS

The Joule heating divided by the coolant mass flow, which is approximately equal to the enthalpy gain of the coolant gas, is plotted on Figure 4 versus $\dot{m}/I$. Data are shown for the second and third designs and for a 2,000-A commercial lead that utilizes a braided conductor. At large values of $\dot{m}/I$ the lead is relatively cool and the I^2R heating is low. As the coolant rate is decreased the lead warms up with a subsequent increase in resistance, and therefore I^2R heating, and a runaway condition is rapidly approached.

The heat transfer in the parallel plate leads is very nearly ideal. That is, the lead and coolant are essentially at the same temperature at any station. Therefore, a good correlation should exist between the lead temperature profile (and therefore its resistance) and the enthalpy gain of the vent gas.

When the lead resistance is plotted versus $I^2R/\dot{m}$ on logarithmic coordinates, a family of straight lines of 2/3 slope results--one for each current. When these data are cross plotted at a fixed value of $I^2R/\dot{m}$, the resistance is found to be inversely related to the current. Combining these relations and defining an average resistivity, $\bar{\rho} = RA/L$, we find

$$\bar{\rho} \propto \frac{IA}{L\dot{m}^2} \qquad (1)$$

and

$$\frac{I^2R}{\dot{m}} \propto (I/\dot{m})^3 \quad . \qquad (2)$$

Plotted on Figure 5 is the measured average resistivity versus $IA/L\dot{m}^2$ for the two LBL-manufactured leads, the commercial 2,000-A lead and some data from Reference 2 which were obtained at the NBS on a braided copper lead. For the commercial lead, A/L was inferred from the room temperature resistance. Note that the correlation does seem to have some applicability to all of these leads. The expectation of higher temperatures, and therefore resistivity, as a result of poorer heat transfer in the commercial and NBS leads is confirmed. Because the majority of the lead resistance is developed near the top of the lead, the data for the tapered lead are correlated based on the area one quarter of the way down from the top. Equation (2) explains the usual qualitative observation of the rapidity with which a current lead will approach runaway as the ratio $I/\dot{m}$ is increased. The $I^2R/\dot{m}$ data shown on Figure 4 for the tapered lead are replotted vs. $\dot{m}/I$ on Figure 6 on logarithmic coordinates. The data are well represented by a straight line with a slope of 3 as predicted by Eq. (2).

The tapered leads have been operated as high as 2,400 A (limit of our power supply) at an $\dot{m}/I$ of 5.9×10^{-5} g/SA. At this point they appeared quite stable with no tendency toward runaway. At 2,000 A they have been operated at an $\dot{m}/I$ as low as 4.3×10^{-5} g/SA, again quite stably. If the ratio $\dot{m}/I$ is reduced below the above values at the stated currents, the leads will very slowly warm up and approach runaway. If at 2,000 A, $\dot{m}/I$ is reduced to 90% of the above value, the leads can be operated for a period on the order of 20 minutes before a dangerous condition is reached.

The pressure loss in the parallel plate leads is relatively high in comparison with most designs. Typically the pressure drop ranges from 20 to 40 mm Hg for the tapered design. For a narrow rectangular channel the laminar flow pressure gradient is

$$\frac{dp}{dx} = \frac{-3\mu\bar{u}}{b^2} \qquad (3)$$

or for N channels of cross section 2b x W

$$\Delta p = \frac{3}{2} \frac{\bar{\nu} L \dot{m}}{N W b^3} \quad . \qquad (4)$$

Because ν is strongly temperature dependent, a correlation should be anticipated between the average values of $\bar{\nu}$ and $\bar{\rho}$. The kinematic viscosity computed from Eq. (4) is plotted versus average resistivity in Figure 7 for the tapered leads. There appears to be an approximately linear relation between $\bar{\nu}$ and $\bar{\rho}$.

NOTATION

a	=	Acoustic velocity
A	=	Conductor area
b	=	Half space between conductors
D_h	=	Hydraulic diameter
I	=	Current
L	=	Cooled length of conductor
$\dot{m}$	=	Coolant mass flow rate

N	=	Number of coolant flow passages
P	=	Pressure
R	=	Resistance
$\bar{u}$	=	Velocity averaged across the flow channel
W	=	Width of flow channel
X	=	Length coordinate
$\bar{\rho}$	=	Average resistivity
Δ	=	$\frac{D_h}{2}\left(\frac{a_c}{\ell_c \nu_c}\right)^{1/2}$
μ	=	Viscosity
$\bar{\nu}$	=	Average kinematic viscosity
ζ	=	Ratio of temperature steplengths in stability model

Subscripts

o	=	Reference value
c	=	Evaluated at cold-end temperature
h	=	Evaluated at warm-end temperature

CONCLUSIONS

A design for a very well behaved copper current lead has been described. A correlation of the experimental data has yielded phenomenological relations that accurately characterize four production samples. It is anticipated that this correlation will also describe the characteristics of other designs of helium-cooled copper current leads, the accuracy of which depends primarily on the degree to which ideal heat transfer is approached. The geometrical dependence of the relations developed must be regarded as tentative since the present data cover only a narrow range.

ACKNOWLEDGMENTS

The author wishes to acknowledge the contributions of others to this work: W. L. Pope, analysis and design; R. V. Schafer, design and fabrication; W. S. Gilbert, J. B. Rechen, W. W. Chupp, and W. I. Lee, testing. This work was done under the auspices of the U. S. Department of Energy.

REFERENCES

1. Rott, N., ZAMP 20 (1969) 230 and ZAMP 24 (1973) 54.
2. Jones, M. C., et al., CONS/3800-1, UC-95W, U. S. National Bureau of Standards (1977).
3. von Hoffman, T., et al., Cryogenics 13 (1973) 490.

FIGURE CAPTIONS

Fig. 1. Stability boundaries from the calculations of Rott.[1]

Fig. 2. Current lead cross section.

Fig. 3. Completed current leads, second and third design.

Fig. 4. Approximate enthalpy gain of vent gas.

Fig. 5. Resistivity correlation.

Fig. 6. Approximate enthalpy gain of vent gas for the tapered lead.

Fig. 7. Average kinematic viscosity for the tapered leads.

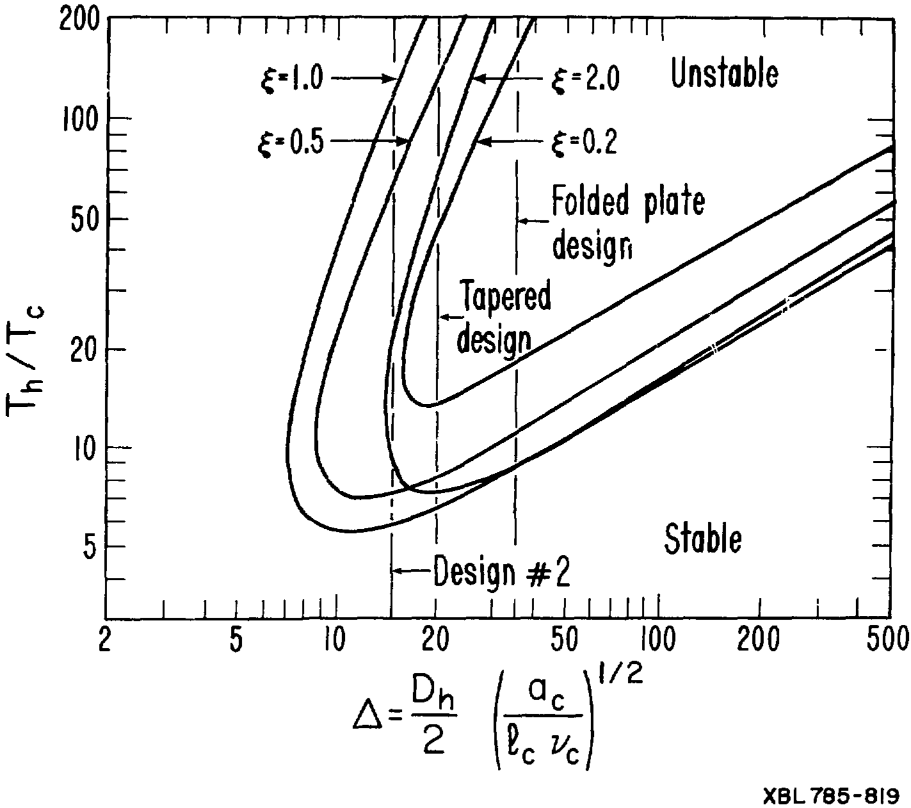

200
100
50
20
10
5
2
5
10
20
50
100
200
500
ξ=1.0
ξ=0.5
ξ=2.0
ξ=0.2
Unstable
Folded plate design
Tapered design
Stable
Design #2
T_h / T_c
$\Delta = \frac{D_h}{2}\left(\frac{a_c}{\ell_c \nu_c}\right)^{1/2}$
XBL 785-819

Fig. 1

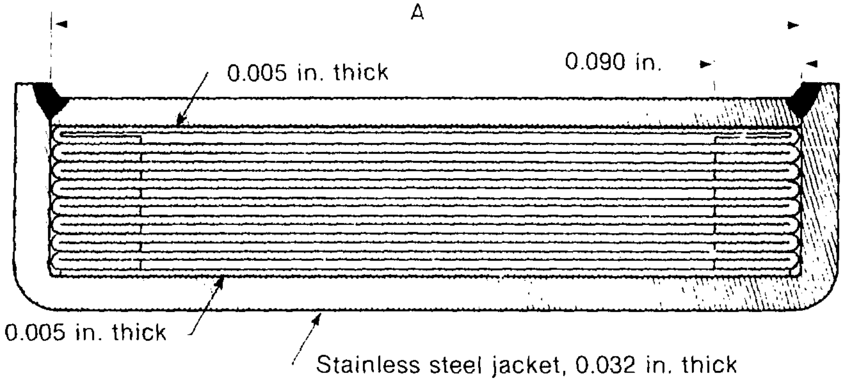

		Non tapered design	Tapered design
Copper cross sectional area (cm^2)	Top	0.474	0.702
	Bottom	0.474	0.365
Number of conductors		9	9
Number of flow channels		8	8
Flow channel dimensions (cm)	Top	1.45 × 0.025	1.92 × 0.032
	Bottom	1.45 × 0.025	0.56 × 0.032
Length of cooled conductor (cm)		63	63
Dimension A (cm)	Top	1.91	2.38
	Bottom	1.91	1.02
Thickness of seven center conductors (cm)		0.025	0.032

XBL 735-977

Fig. 2

Fig. 3

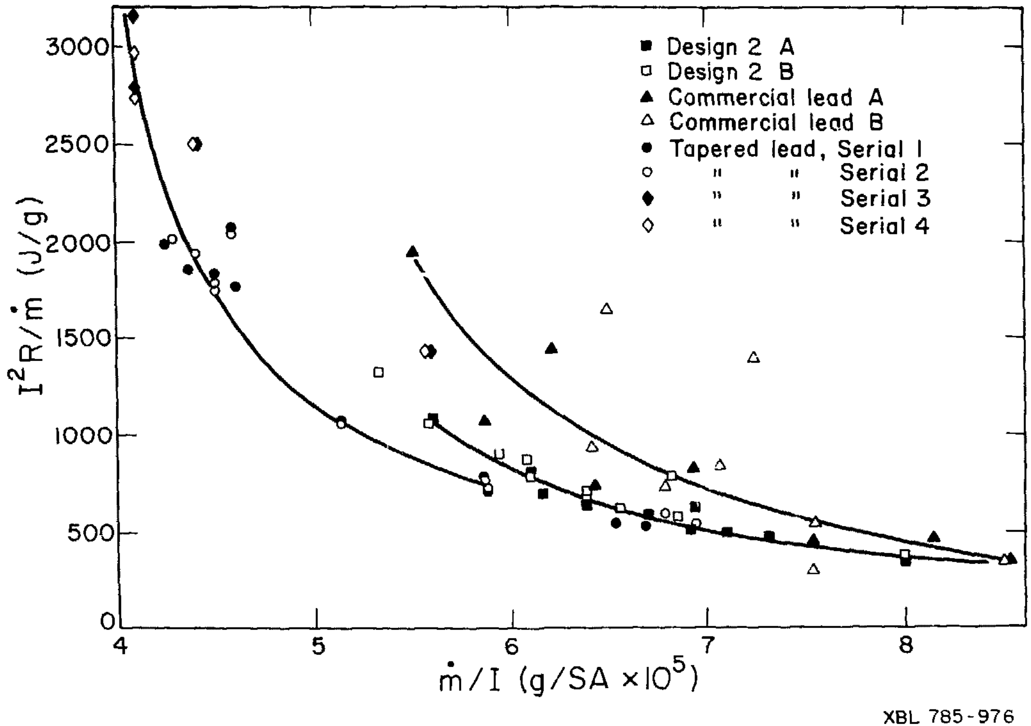

Design 2 A
Design 2 B
Commercial lead A
Commercial lead B
Tapered lead, Serial 1
" " Serial 2
" " Serial 3
" " Serial 4
3000
2500
2000
1500
1000
500
0
4
5
6
7
8
$I^2R/\dot{m}$ (J/g)
$\dot{m}/I$ (g/SA $\times 10^5$)
XBL 785-976

Fig. 4

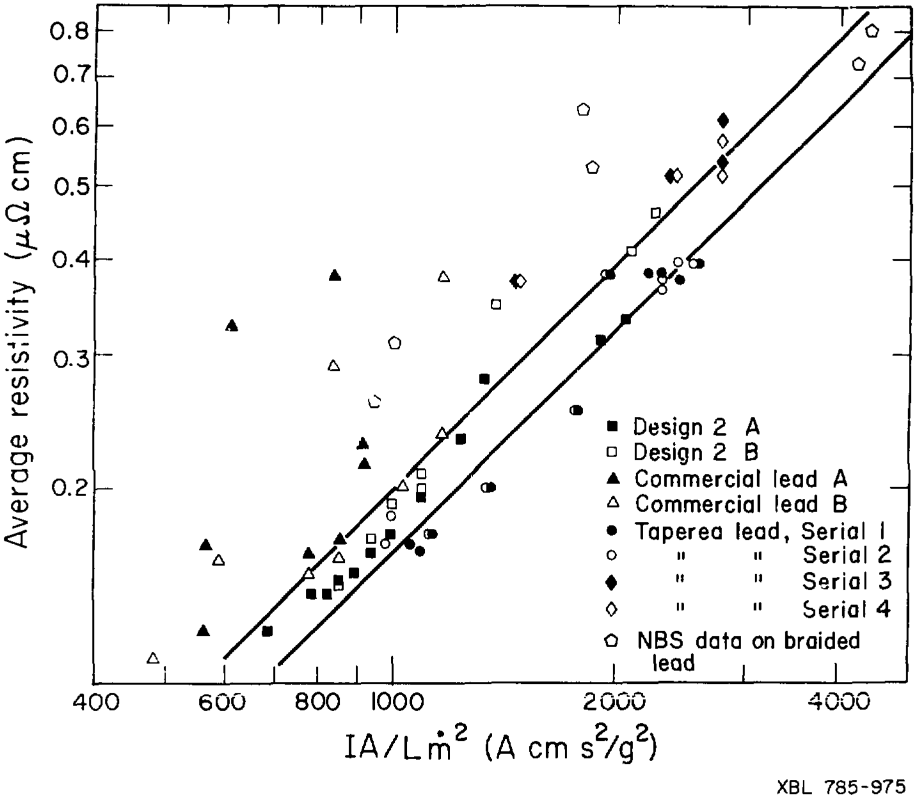

Average resistivity (μΩ cm)
0.8
0.7
0.6
0.5
0.4
0.3
0.2
400
600
800
1000
2000
4000
IA/Lṁ² (A cm s²/g²)
Design 2 A
Design 2 B
Commercial lead A
Commercial lead B
Tapered lead, Serial 1
" " Serial 2
" " Serial 3
" " Serial 4
NBS data on braided lead
XBL 785-975

Fig. 5

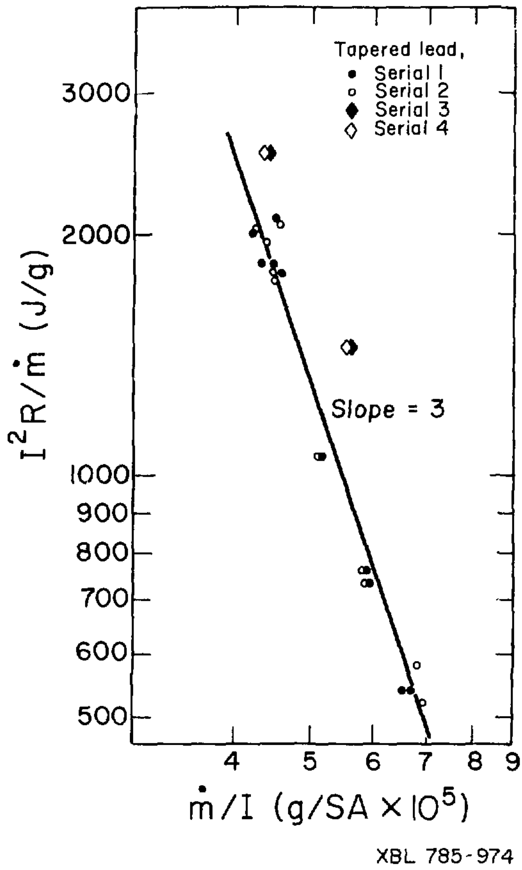
Tapered lead,
Serial 1
Serial 2
Serial 3
Serial 4
3000
2000
1000
900
800
700
600
500
I2R/ṁ (J/g)
Slope = 3
4
5
6
7
8
9
ṁ/I (g/SA × 10^5)
XBL 785-974

Fig. 6

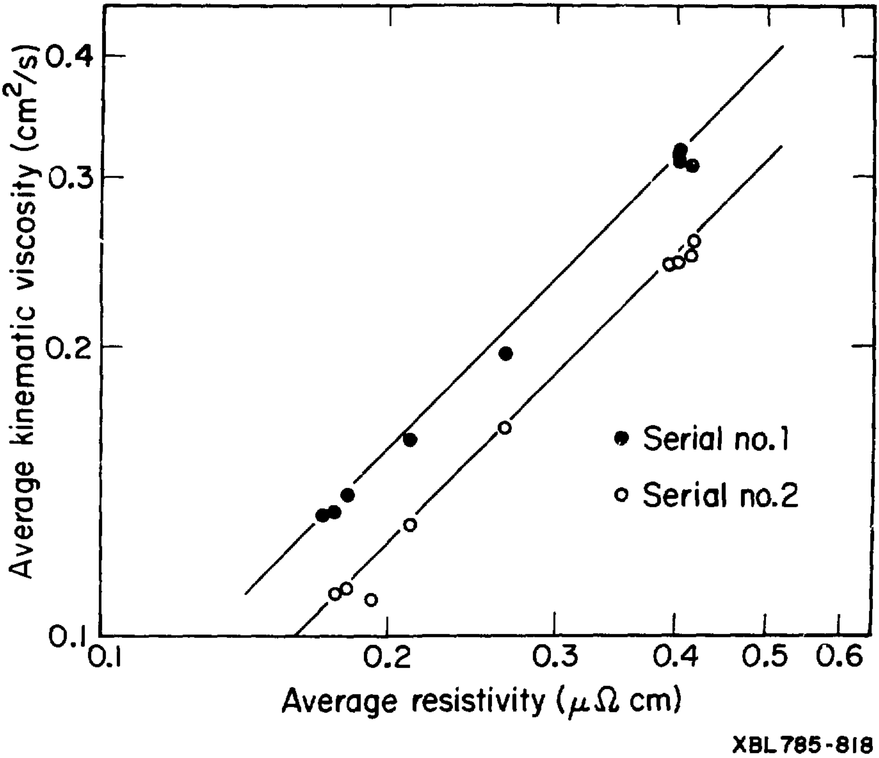
Average kinematic viscosity (cm²/s)
0.4
0.3
0.2
0.1
0.1
0.2
0.3
0.4
0.5
0.6
Average resistivity (μΩ cm)
Serial no.1
Serial no.2
XBL785-818

Fig. .